



This is a repository copy of *Evaluation of High Impedance Surfaces for MRI RF Coil Applications Simulations of RF Field and Specific Absorption Rate*.

White Rose Research Online URL for this paper:

<https://eprints.whiterose.ac.uk/121846/>

Version: Accepted Version

---

**Proceedings Paper:**

Issa, I., Ford, K.L. orcid.org/0000-0002-1080-6193, Rao, M. et al. (1 more author) (2016) Evaluation of High Impedance Surfaces for MRI RF Coil Applications Simulations of RF Field and Specific Absorption Rate. In: 2016 10th European Conference on Antennas and Propagation (EuCAP). 2016 10th European Conference on Antennas and Propagation (EuCAP), 10-15 Apr 2016, Davos, Switzerland. IEEE . ISBN 978-8-8907-0186-3

<https://doi.org/10.1109/EuCAP.2016.7481761>

---

© 2016 IEEE. Personal use of this material is permitted. Permission from IEEE must be obtained for all other users, including reprinting/ republishing this material for advertising or promotional purposes, creating new collective works for resale or redistribution to servers or lists, or reuse of any copyrighted components of this work in other works.

**Reuse**

Items deposited in White Rose Research Online are protected by copyright, with all rights reserved unless indicated otherwise. They may be downloaded and/or printed for private study, or other acts as permitted by national copyright laws. The publisher or other rights holders may allow further reproduction and re-use of the full text version. This is indicated by the licence information on the White Rose Research Online record for the item.

**Takedown**

If you consider content in White Rose Research Online to be in breach of UK law, please notify us by emailing [eprints@whiterose.ac.uk](mailto:eprints@whiterose.ac.uk) including the URL of the record and the reason for the withdrawal request.



[eprints@whiterose.ac.uk](mailto:eprints@whiterose.ac.uk)  
<https://eprints.whiterose.ac.uk/>

# Evaluation of High Impedance Surfaces for MRI RF Coil Applications - Simulations of RF Field and Specific Absorption Rate

Ismail Issa<sup>1</sup>, Kenneth Lee Ford<sup>1</sup>, Madhwesha Rao<sup>2</sup>, James Wild<sup>2</sup>

<sup>1</sup>Department of Electronic and Electrical Engineering, University of Sheffield, Sheffield, UK

<sup>2</sup>Department of Academic Radiology, University of Sheffield, Sheffield, UK

**Abstract**—This paper investigates the use of High Impedance Surfaces (HIS) to enhance the magnetic near-field within a dielectric phantom stimulated by a surface coil antenna resonating at 63.8 MHz for use in Magnetic Resonance Imaging (MRI) systems. Specifically, the optimization of the space between the surface of the coil and the HIS is presented here. The HIS incorporates interdigitated capacitive elements that produce an electrically small unit cell size. The magnetic field strength is shown to be improved by 42% as compared to a system which uses only an RF shield. The associated Specific Absorption Rate (SAR) for the optimum design is simulated and compared to international standards. The work is aimed at 1.5T MRI applications.

**Index Terms**—High Impedance Surface, Magnetic Resonance, Specific Absorption Rate.

## I. INTRODUCTION

Magnetic Resonance Imaging (MRI) is a diagnostic medical imaging technique which yields images from biological tissue based on Nuclear Magnetic Resonance (NMR) phenomenon. Radio Frequency (RF) coils which are tuned to the Larmor frequency are used to excite the nuclear spins and detect the transverse magnetization from their free induction decay. The Larmor frequency can be calculated using (1), [1].

$$f = \frac{\gamma B_0}{2\pi} \quad (1)$$

where  $\gamma$  is the gyromagnetic ratio ( $\gamma/2\pi = 42.58 \text{ MHz/T}$  for hydrogen nuclei,  $^1\text{H}$ ) and  $B_0$  is the static magnetic field of the MRI scanner and the gyromagnetic ratio is dependent on the nuclei of interest. In this paper the interest is in 1.5T MRI systems which is typical for most clinical systems and gives a Larmor frequency of 63.87MHz.

The RF coil is positioned such that the magnetic polarity is perpendicular to the axis of the cylindrical RF shield that lines the bore of the MRI scanner. The RF shield is a high-pass structure which permits low frequency gradient magnetic fields and blocks high frequency components, at a typical Larmor frequency of  $^1\text{H}$ , the RF shield thus it can be approximated to a Perfect Electrical Conductor (PEC), [1]. The radio frequency current induced in the RF coil by the sample is typically reduced because of the out of phase currents caused by the RF shield, this leads to a reduction in Signal to Noise Ratio (SNR) of the received signal and thus, lowers the MRI image quality. In recent years, there has been some interest in using

metamaterials to increase the strength of the RF magnetic field in MRI systems, in order to improve image SNR and quality. A metamaterial is a periodic array of metallic or dielectric elements, which produce electromagnetic properties not found in homogeneous materials. In recent metamaterial research, [2], the authors proposed using a Magneto Inductive (MI) lens to improve the SNR of images obtained with a 7T MRI system using a simple RF surface coil. However, performance at lower resonant frequencies required for 1.5T and 3T MR systems were not found to be as encouraging. A High Impedance Surface (HIS) is an Artificial Magnetic Conductor (AMC), [3], which has properties of in-phase reflection coefficient, which can be used to enhance the radio frequency magnetic field. In, [4], the use of HIS was investigated on a 7T MRI system operating at 300MHz which used electrically small HIS unit cells of only 7.5% of the free space wavelength. By using this method the SNR was improved by 47%. A more recent study using a HIS demonstrated how the spacing between the RF coil and the phantom could be optimized to improve the RF magnetic field, [5]. By using a HIS as an RF shield at 300MHz the magnetic flux density was improved for a small separation distance between the dipole coil and HIS however, the improvement at the higher separation distance was not as marked. The challenge for successful implementation of HIS at lower frequencies (60-130 MHz), is the design of miniaturized HIS unit cell dimensions. Our recent work, [6], proposed a miniaturization technique which was based on an interdigital capacitor approach, [7], and was demonstrated at 63.8MHz. In this paper we investigate, through numerical simulations, the optimum spacing between a HIS, based on our previous design approach, and a RF surface coil which is spaced close to a dielectric phantom that mimics the properties of the human body. The aim of work is to increase the strength of the RF magnetic field as compared to the case when a HIS is not employed. Additionally, the Specific Absorption Rate (SAR) inside the phantom is simulated and verified against regulatory standards such as IEC60604-2-33/2010, [8].

## II. MRI CONCEPT AND HIS DESIGN

The concept of interest is illustrated in Fig.1. A PEC RF shield is placed a distance of  $t=100\text{mm}$  away from a capacitive layer which forms the HIS. The choice of the spacing,  $t$ , is

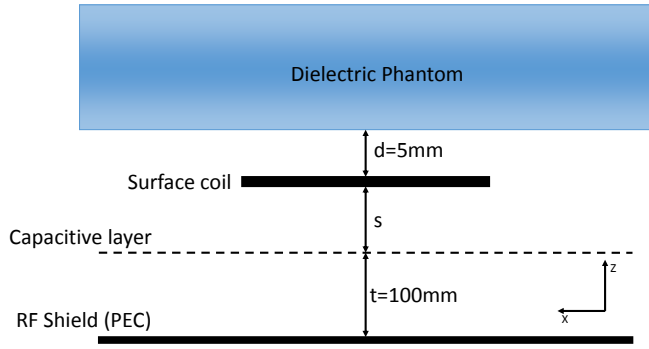


Fig. 1. MRI concept

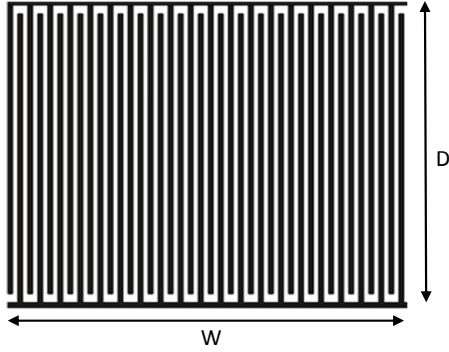


Fig. 2. Unit cell of capacitive layer

commensurate with the available space that may be found in the bore of a clinical MRI scanner.

A resonant RF surface coil was designed and simulated in [6] and is used here as a transceiver operating at a Larmor frequency of 63.8MHz which is appropriate for imaging the 1H nuclear magnetic resonance on a 1.5T MRI system. As a simple model of the load of the human body at 63.8MHz, a homogeneous phantom with dimensions length=335mm, width=230mm, height=140mm, ( $\epsilon_r = 65, \sigma = 0.4S/m$ ), [9], [10] was placed 5mm above the loop coil which is similar to those used for surface imaging on clinical MRI systems. Fig. 2, illustrates the proposed unit cell of the capacitive layer which comprises of inter-digital metallic elements digits where the digit width is equal to the spacing between digits. This unit cell geometry was chosen as it provides a high capacitance density in order to maximize the capacitance density [7]. The dimensions are illustrated in Fig 2, and it was assumed that the capacitive layer has a 1.6mm thick FR4 substrate ( $\epsilon_r = 4.3, \tan \delta = 0.025$ ). The design of the HIS was carried out using approximations for interdigital capacitance, [6], [7], shown in [11] by (2). This can then be combined with the equivalent inductance of the space between the RF shield and the capacitive layer,  $L=t$  to find the resonant frequency of the HIS, given by (3).

$$C = \frac{\epsilon_{eff} * 10^{-3}(N-1)D}{18\pi} \frac{K(k)}{K'(k)} pF \quad (2)$$

$$f = \frac{1}{2\pi\sqrt{LC}} \quad (3)$$

Where  $K(k)$  is the complete elliptic integral and  $K'(k)$  is its compliment,  $D$  is the digit length,  $N$  is the number of digits and  $\epsilon_{eff} = \frac{\epsilon_r + 1}{2}$ . It can be shown that  $\frac{K(k)}{K'(k)} = 0.5$  if the digit width and the spacing between the digits are equal.

The proposed HIS dimensions are  $D=50mm, W=56mm$  with a 1mm gap between the end of the digits and the metallic horizontal strip. The number of digits,  $N$ , is 40, the width of each digit is 0.7mm and the spacing between digits is 0.7mm. In order to reduce simulation time for the scenario shown in Fig. 1, the capacitive layer was implemented as an effective surface impedance. The surface impedance was determined by simulating the S-parameters of the inter-digital unit cell, including PEC, and then converting this to an input impedance using CST microwave studio. Following this the equivalent complex impedance of the capacitive layer may be de-embedded from the impedance of the PEC shield.

### III. NUMERICAL SIMULATIONS

#### A. Radio Frequency Magnetic Field Improvement

CST simulations were carried out for the model in Fig. 1 where the magnitude of the magnetic field inside the phantom was monitored, along the x-axis ( $z=45mm$ ). The effect of a variation of the separation distance,  $s$ , between the RF coil and the capacitive layer was investigated to provide the largest magnetic field when the surface coil had a 1A sinusoidal current source at 63.8MHz. Fig.3 shows that for an increased or decreased separation value between the RF coil and the capacitor layer greater than or less than 5mm, the strength of the magnetic field is reduced inside the phantom, whereas the highest value occurs for  $s=5mm$ .

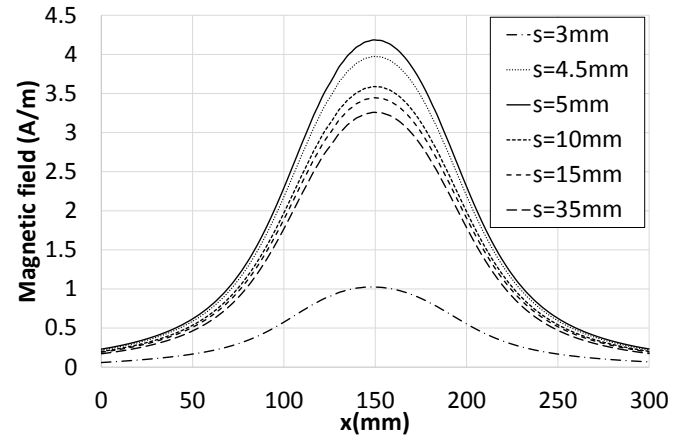


Fig. 3. Simulated  $H_1$ -field at 45mm above the RF coil for varying separation,  $s$ , between the coil and HIS.

Figs. 4 and 5 present the absolute value of the magnetic and electric fields at the optimal coil separation value of  $s=5mm$  in the transverse cut-plane (x-axis). Data is presented for the

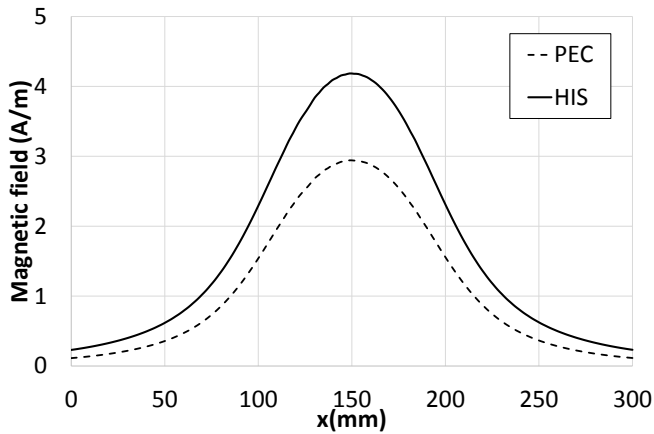


Fig. 4. Simulated  $H_1$ -field at 45mm above the RF coil at  $s=5$ mm, with and without the HIS.

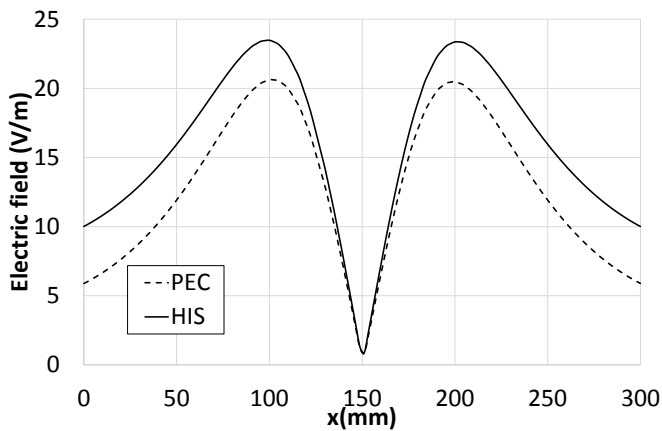


Fig. 5. Simulated magnitude of E-field at 45 mm above the RF coil at  $s=5$  mm with and without the HIS.

cases both with and without the capacitive layer for comparison. Fig. 4 shows that there is an improvement in the  $H_1$  field of approximately 42% when compared to the PEC case at the center position,  $x=150$ mm. This improvement is due to the in-phase reflection from the HIS ground plane. Fig. 5 shows that the magnitude of the electric field is also increased when compared to the PEC case by approximately 14% at the maximum E-field position ( $x=100$ mm or  $x=200$ mm). Due to this increase in E-field the effect on the SAR was then investigated further.

### B. Specific Absorption Rate

The SAR is investigated inside the homogeneous dielectric phantom for the cases of with and without the capacitive layer. All values of SAR have been normalized to a 1W transmission power. Following the full field simulations the values for the maximum 10g sample in the phantom and the whole body SAR were calculated using the in-built facility in CST. The simulated SAR values for the maximum 10g case were 5.6W/kg and 3.3W/kg for the capacitive layer and without capacitive layer respectively. The maximum value allowed by

the IEC60604-2-33/2010 standard is 10W/kg. The whole body SAR was 0.26W/kg and 0.11W/kg for the capacitive layer and without capacitive layer respectively which can be compared to the IEC standard of 2W/kg.

## IV. CONCLUSION

In this paper we demonstrated an approach to enhance the magnitude of the radio frequency magnetic field of a RF loop coil above a high impedance surface for MRI applications. The results show that the HIS can improve the  $H_1$ -field by approximately 42% when compared to the PEC case at the center of a dielectric phantom. However, the HIS also causes a concomitant increase in the electric field by 14%, which leads to an increase in SAR when compared to the PEC case. According to the aforementioned SAR guidelines, the SAR values for both the RF shield and HIS ground planes in this study are below the maximum allowed SAR values. A possible alternative for our approach would be in a receive only application which will be investigated in future work.

## REFERENCES

- [1] J. T. Vaughan and J. R. Griffiths, *RF Coils for MRI*. Wiley, 2012.
- [2] J. M. Algarín, M. J. Freire, F. Breuer, and V. C. Behr, "Metamaterial magnetoinductive lens performance as a function of field strength," *Journal of Magnetic Resonance*, vol. 247, pp. 9–14, 2014.
- [3] D. Sievenpiper, L. Zhang, R. F. J. Broas, N. G. Alexopolous, and E. Yablonovitch, "High-impedance electromagnetic surfaces with a forbidden frequency band," *IEEE Transactions on Microwave Theory and Techniques*, vol. 48, no. 4, p. 620, 2000.
- [4] G. Saleh, K. Solbach, and A. Rennings, "EBG structure to improve the B1 efficiency of stripline coil for 7 Tesla MRI," in *Proceedings of 6th European Conference on Antennas and Propagation, EuCAP 2012*, 2012, pp. 1399–1401.
- [5] Z. Chen, K. Solbach, D. Erni, and A. Rennings, "Improved B1 distribution of an MRI RF coil element using a high-impedance-surface shield," in *Microwave Conference (GeMiC), 2015 German*, 2015, pp. 111–114.
- [6] I. Issa, K. Ford, M. Rao, and J. Wild, "A High Impedance Surface for Improving the Radio Frequency Magnetic Field for a 1.5 Tesla Magnetic Resonance System," in *Loughborough Antennas and Propagation Conference, LAPC 2015, In press*, 2015.
- [7] R. Saad and K. L. Ford, "A miniaturised dual band artificial magnetic conductor using interdigital capacitance," in *Antennas and Propagation (EuCAP), 2014 8th European Conference on*, 2014, pp. 25–26.
- [8] *IEC 60601-2-33: Particular requirements for the basic safety and essential performance of magnetic resonance equipment for medical diagnosis*, IEC Std., 2010.
- [9] M. Stuchly and S. Stuchly, "Dielectric properties of biological substances-tabulated," *Journal of Microwave Power*, vol. 15, pp. 19–26, 1980.
- [10] K. R. Foster and H. P. Schwan, "Dielectric properties of tissues and biological materials: a critical review." *Critical Reviews in Biomedical Engineering*, vol. 17, no. 1, pp. 25–104, 1989.
- [11] I. J. Bahl, *Lumped Elements for RF and Microwave Circuits*. Artech House, 2003.